Edges and Corners with Shearlets

Miguel A. Duval-Poo, Francesca Odone, and Ernesto De Vito

***Abstract*—Shearlets are a relatively new and very effective multi-scale framework for signal analysis. Contrary to traditional wavelets, shearlets are capable to efficiently capture the anisotropic information in multivariate problem classes. Therefore, shearlets can be seen as the valid choice for multi-scale analysis and detection of directional sensitive visual features like edges and corners. In this paper we we start by reviewing the main properties of shearlets that are important for edge and corner detection. Then we study algorithms for multi-scale edge and corner detection based on the shearlet representation. We provide an extensive experimental assessment on benchmark datasets which empirically confirms the potential of shearlets feature detection.**

***Index Terms*—Shearlets, multi-scale image analysis, image features, edge detection, corner detection.**

I. Introduction

FEATURE detection is an important problem of early vision. The feature detection process consists in the extraction of *perceptually interesting* low level features over an image, preparing it to further higher level processing tasks such as image registration, image matching, image classification or retrieval, just to name a few. Multi-scale image representations [1]–[3] provide the framework for detecting features at coarse and fine scale simultaneously and, to some extent, to devise scale invariant image descriptors. Of particular interest for our work are multi-scale methods based on wavelets, which have been successfully applied to the analysis and detection of features like edges [4], [5] and corners [6]–[8]. However, wavelets are known to have a limited capability in dealing with directional information. In recent years, several methods like contourlets [9], complex wavelets [10], ridgelets [11], curvelets [12], and shearlets [13], were introduced to overcome these limitations. Compared to all these methods, the shearlet representation stands out since it offers a unique combination of some highly desirable properties: it has a single or finite set of generating functions, it provides optimally sparse representations for a large class of multidimensional data, it allows the use of compactly supported analyzing functions both in the space and frequency domain. Last, but not less important, it has fast algorithmic implementations and it allows a unified treatment of the continuum and digital realms. For these reasons, in this work we choose shearlets as a reference framework for feature detection.

In this paper we first review the shearlet transform focusing on the problem of edge and corner detection. Then, we propose algorithms for multi-scale edge and corner detection in images. We take inspiration from [14] and [15], but we adopt a different algorithm to compute the digitalized shearlet transform, which was first introduced in [16], [17] for segmentation problems. With respect to the latter references we choose a *mother function* suitable for signal discontinuities enhancement [5].

In this work we consider a classical setting, where the mother shearlet factorizes in the Fourier domain as the product of a one-dimensional wavelet and a bump functions. The review paper [18] shows the effectiveness of this choice in many problems in image processing. An alternative construction has been proposed in [19] where the mother shearlet has compact support in the space domain. We refer to [20] for a discussion on the differences between the two approaches and to [21] for the algorithm issues.

For edge detection we consider two computational procedures: the shearlet cascade algorithm (SCED) introduced in [15] and the shearlet multiplicative algorithm (SMED), which was originally proposed for wavelets [22]. As for corner detection, we propose a new procedure inspired by [23] and based on the notion of *cornerness*.

We experimentally assess the proposed feature detection algorithms on benchmark data-sets of real images, the Berkeley Segmentation Dataset (BSDS300) [24] and the Oxford evaluation benchmark [25]. The experimental analysis is in fact a further contribution of the paper, since previous works applying shearlets to feature detection problems lacked an extensive experimental analysis on large and complex sets of real images. The obtained results show the ability of the shearlet representation to encode low level features that are relevant for singularity detection and highlight how the directional informational available in the shearlet coefficients can be beneficial for the edge/corner detection procedures.

The remainder of this paper is organized as follows: in Section II we review the shearlet transform in the continuous and discrete case and provide a computational complexity analysis. Section III and Section IV respectively propose edge detection and corner detection algorithms. Section V reports a detailed experimental analysis of edge detection on the Berkeley dataset and corner detection following the Oxford evaluation procedure. Section VI is left to a final discussion.

II. A Review of the Shearlet Transform

Shearlets are a relatively new class of multidimensional representation systems, capable of efficiently encoding anisotropic features in multivariate data. They are a natural extension of wavelets able to overcome wavelet inability of capturing anisotropic features. In this section we review the main properties of shearlets, referring the interested reader to [13], [26]–[29].

M.A. Duval-Poo and F. Odone are with the Dipartimento di Informatica Bioingegneria Robotica e Ingegneria dei Sistemi (DIBRIS), Università degli Studi di Genova, 16146 Genova, Italy (e-mail: miguel.duval.poo@dibris.unige.it; francesca.odone@unige.it).

E. De Vito (corresponding author) is with the Dipartimento di Matematica (DIMA), Università degli Studi di Genova, 16146 Genova, Italy (e-mail: devito@dima.unige.it).

A shearlet is generated by the dilation, shearing and translation of a function $\psi \in L^2(\mathbb{R}^2)$, called the *mother shearlet*, in the following way

$$\psi_{a,s,t}(x) = a^{-3/4}\psi(A_a^{-1}S_s^{-1}(x-t)) \tag{1}$$

where $t \in \mathbb{R}^2$ is a translation, A_a is a *scaling* (or *dilation*) matrix and S_s a *shearing* matrix defined respectively by

$$A_a = \begin{pmatrix} a & 0 \\ 0 & \sqrt{a} \end{pmatrix} \qquad S_s = \begin{pmatrix} 1 & -s \\ 0 & 1 \end{pmatrix},$$

with $a \in \mathbb{R}^+$ and $s \in \mathbb{R}$. The anisotropic dilation A_a controls the scale of the shearlets, by applying a different dilation factor along the two axes. The shearing matrix S_s, not expansive, determines the orientation of the shearlets. The normalization factor $a^{-3/4}$ ensures that $\|\psi_{a,s,t}\| = \|\psi\|$, where $\|\psi\|$ is the norm in $L^2(\mathbb{R}^2)$.

In the classical setting the *mother shearlet* ψ is assumed to factorize in the Fourier domain as

$$\hat{\psi}(\omega_1, \omega_2) = \hat{\psi}_1(\omega_1)\hat{\psi}_2(\frac{\omega_2}{\omega_1}) \tag{2}$$

where $\hat{\psi}$ is the Fourier transform of ψ, ψ_1 is a one dimensional wavelet and $\hat{\psi}_2$ is any non-zero square-integrable function. There are several examples of functions ψ_1, ψ_2 satisfying these properties. In Section III we will discuss an appropriate mother function for edge and corner detection. With the choice of Equation (2) the shearlet definition in the frequency domain becomes

$$\hat{\psi}_{a,s,t}(\omega_1, \omega_2) = a^{3/4}\hat{\psi}_1(a\omega_1)\hat{\psi}_2\left(\frac{\omega_2 - s\omega_1}{\sqrt{a}\,\omega_1}\right) e^{-2\pi i(\omega_1,\omega_2)\cdot t}. \tag{3}$$

The *shearlet transform* $\mathcal{SH}(f)$ of a signal $f \in L^2(\mathbb{R}^2)$ is defined by

$$\mathcal{SH}(f)(a, s, t) = \langle f, \psi_{a,s,t}\rangle, \tag{4}$$

where $\langle f, \psi_{a,s,t}\rangle$ is the scalar product in $L^2(\mathbb{R}^2)$. As a consequence of the Plancherel formula, Equation (4) can be rewritten as

$$\mathcal{SH}(f)(a, s, t) = a^{3/4} \int_{\hat{R}^2} \hat{f}(\omega_1, \omega_2)\hat{\psi}_1(a\omega_1)\times \hat{\psi}_2\left(\frac{\omega_2 - s\omega_1}{\sqrt{a}\,\omega_1}\right) \times e^{2\pi i t\cdot(\omega_1,\omega_2)} d\omega_1 d\omega_2.$$

A. Shearlets reponse to singular points

The continuous shearlet transform is able to capture the geometry of edge singularities through its asymptotic decay at fine scales ($a \to 0$). A group of theoretical results [15], [18], [27], [29] show that the continuous shearlet transform precisely describes the geometric information of edges and other singular points of an image through their asymptotic behavior at fine scales. These results can be summarized as follows.

Let an image $\mathcal{I}$ be modeled as piecewise smooth function in $\Omega = [0, 1]^2$. That is, its assumed that $\mathcal{I}$ is smooth everywhere on Ω, except for a collection of finitely many piecewise smooth curves, denoted by Γ, where jump discontinuities may occur. Then, the asymptotic decay properties of the continuous shearlet transform $\mathcal{SH}$ of $\mathcal{I}$ can be defined as follows [30]:

- If a point $t \notin \Gamma$, then $|\mathcal{SH}(\mathcal{I})(a, s, t)|$ decays rapidly [1], as $a \to 0$, for each $s \in \mathbb{R}$.
- If a point $t \in \Gamma$ and Γ is smooth near t, then $|\mathcal{SH}(\mathcal{I})(a, s, t)|$ decays rapidly, as $a \to 0$, for each $s \in \mathbb{R}$ unless $s = s_0$ is the normal orientation to Γ at t. For $s = s_0$, $|\mathcal{SH}(\mathcal{I})(a, s_0, t)| \sim a^{3/4}$, as $a \to 0$.
- If a point t is a corner point of Γ and $s = s_0$, $s = s_1$ are the normal orientations to Γ at t, then $|\mathcal{SH}(\mathcal{I})(a, s_0, t)|, |\mathcal{SH}(\mathcal{I})(a, s_1, t)| \sim a^{3/4}$, as $a \to 0$. For all other orientations, the asymptotic decay of $|\mathcal{SH}(\mathcal{I})(a, s, t)|$ is faster (even if not necessarily *rapid*).

In a recent pre-print [31] a similar behaviour is obtained by using compactly supported shearlets.

In addition, spike singularities (noise points) produce a very different behavior than jump discontinuities on the decay of the continuous shearlet transform. Let us consider a Dirac delta distribution centered at $t_0 \in \mathbb{R}$. Then

$$|\mathcal{SH}(\delta_{t_0})(a, s, t_0)| \asymp s^{-3/4}, \quad \text{as } a \to 0.$$

that is, the continuous shearlet transform of δ_{t_0}, at $t = t_0$ increases at fine scales. The decay is rapid for $t \neq t_0$. We stress that the above results hold provided that ψ_1 and ψ_2 satisfy some additional condition we will discuss in Section III-A.

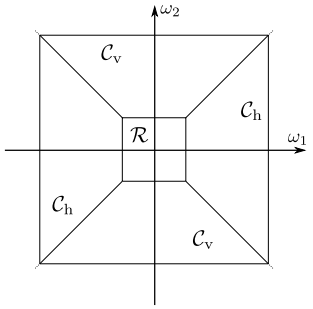

Fig. 1. Decomposition of the frequency domain into cones.

B. Cone-adapted Shearlets

A major limitation of the shearlets defined in the previous section is the directional bias of shearlet elements associated with large shearing parameters. A common way to deal with this problem is to partition the Fourier domain into four cones, and separate the low-frequency region by cutting out a square centered around the origin. This yields a partition of the frequency plane as illustrated in Fig. 1. This concept is commonly known as *cone-adapted shearlets* and was introduced in [13]. It can be seen that within each cone, the shearing parameter s is only allowed to vary over a finite range, therefore, this produces elements whose orientations are distributed more uniformly. This fact has certain advantages for numerical implementation.

[1]Here *rapid decay* means that for any $N \in \mathbb{N}$, there is a $C_N > 0$ such that $|\mathcal{SH}(\mathcal{I})(a, s, t)| \leq C_N a^N, \quad \text{as } a \to 0.$

Formally, the two conic regions are defined as

$$\mathcal{C}_{\mathrm{h}} = \{(\omega_1, \omega_2) \in \mathbb{R}^2 : |\omega_2/\omega_1| \leq 1, |\omega_1| > 1\}$$
$$\mathcal{C}_{\mathrm{v}} = \{(\omega_1, \omega_2) \in \mathbb{R}^2 : |\omega_1/\omega_2| \leq 1, |\omega_2| > 1\}$$

and the low-frequency part as

$$\mathcal{R} = \{(\omega_1, \omega_2) \in \mathbb{R}^2 : |\omega_1|, |\omega_2| \leq 1\}.$$

Let, for each set $\mathcal{C}_x, x \in \{\mathrm{h}, \mathrm{v}\}$, be defined a cut-off function $\chi_{\mathcal{C}_{\mathrm{h}}}(\omega)$ which is equal to 1 for $\omega \in \mathcal{C}_x$ and 0 for $\omega \notin \mathcal{C}_x$. Then, the shearlet ψ can be suited for the horizontal cone as

$$\hat{\psi}^h(\omega_1, \omega_2) = \hat{\psi}_1(\omega_1)\hat{\psi}_2\left(\frac{\omega_2}{\omega_1}\right)\chi_{\mathcal{C}_{\mathrm{h}}}.$$

Analogously the shearlet for the vertical cone can be defined, where the roles of ω_1 and ω_2 are interchanged, i.e.

$$\hat{\psi}^v(\omega_1, \omega_2) = \hat{\psi}_1(\omega_2)\hat{\psi}_2\left(\frac{\omega_1}{\omega_2}\right)\chi_{\mathcal{C}_{\mathrm{v}}}.$$

The remaining part $\mathcal{R}$ can be handled by a scaling function $\hat{\phi}(\omega_1, \omega_2)$.

C. Digital Shearlets

Digital shearlet systems are defined by sampling continuous shearlet systems on a discrete subset of the space of parameters $\mathbb{R}_+ \times \mathbb{R}^3$ and by sampling the signal on a grid. It is reasonable to expect that the resulting discrete systems will inherit some basic geometric properties of the corresponding continuous systems and, thus, their ability to localize spatially distributed discontinuities. In the literature there are many different discretization schemes, see [21] and reference therein.

In this paper we adopt the Fast Finite Shearlet Transform (FFST) [16] which performs the entire shearlet construction in the Fourier domain. This implementation is computationally more efficient than analysis performed in the space domain, unless ad hoc optimizations are applied, and allows us to obtain algorithms that follow exactly the theoretical conceptual path: this is a benefit in terms of elegance and clarity of the implementation. In this scheme, the signal is discretized on a square on size N, which is independent of the dilation and shearing parameter, whereas the scaling, shear and translation parameters are discretized as

$$a_j = 2^{-j}, \quad j = 0, \ldots, j_0 - 1,$$
$$s_{j,k} = k2^{-j/2}, \quad -\lfloor 2^{j/2} \rfloor \leq k \leq \lfloor 2^{j/2} \rfloor,$$
$$t_m = \left(\frac{m_1}{N}, \frac{m_2}{N}\right), \quad m \in \mathcal{I}$$

where j_0 is the number of considered scales and $\mathcal{I} = \{(m_1, m_2) : m_1, m_2 = 0, \ldots, N-1\}$. With respect to the original implementation we use a dyadic scale 2^{-j} instead of 4^{-j} to reduce the difference among two consecutive scales. With these notations the shearlet system becomes

$$\psi^{\mathrm{x}}_{j,k,m}(x) = \psi^{\mathrm{x}}_{a_j, s_{j,k}, t_m}(x)$$

where $\mathrm{x} = \mathrm{h}$ or $\mathrm{x} = \mathrm{v}$. In the Fourier domain it becomes

$$\hat{\psi}^{\mathrm{h}}_{j,k,m}(\omega_1, \omega_2) = 2^{\frac{3j}{4}}\hat{\psi}_1(2^{-j}\omega_1)\hat{\psi}_2\left(2^{\frac{j}{2}}\frac{\omega_2}{\omega_1} - k\right) \times \\ \times e^{-2\pi i \frac{\omega_1 m_1 + \omega_2 m_2}{N}}\chi_{\mathcal{C}_{\mathrm{h}}}(\omega_1, \omega_2) \quad (5)$$

where

$$(\omega_1, \omega_2) \in \{(\omega_1, \omega_2) : \omega_1, \omega_2 = -\lfloor \frac{N}{2} \rfloor, \ldots, \lceil \frac{N}{2} \rceil - 1\}.$$

If $\mathrm{x} = \mathrm{v}$ we have a similar formula by interchanging ω_1 and ω_2. Note that, if the scale j is fixed we can remove the normalization factor $2^{\frac{3j}{4}}$ in (5).

Finally, for the low frequency domain, we set

$$\phi_m(x) = \phi(x - t_m),$$
$$\hat{\phi}_m(\omega) = \hat{\phi}_m(\omega_1, \omega_2)\, e^{-2\pi i \frac{\omega_1 m_1 + \omega_2 m_2}{N}}.$$

The discrete shearlet transform of an digital image $\mathcal{I}$ is now defined as

$$\mathcal{SH}(\mathcal{I})(j,k,m) = \begin{cases} \langle \mathcal{I}, \phi_m \rangle \\ \langle \mathcal{I}, \psi^h_{j,k,m} \rangle \\ \langle \mathcal{I}, \psi^v_{j,k,m} \rangle \end{cases}$$

where $j = 0, \ldots, j_0 - 1$, $|k| \leq \lfloor 2^{j/2} \rfloor$, $m \in \mathcal{I}$. Based on the Plancherel formula $\langle f, g \rangle = \frac{1}{MN}\langle \hat{f}, \hat{g} \rangle$, the discrete shearlet transform can be efficiently computed by applying the 2D Fast Fourier Transform (`fft`) and its inverse (`ifft`). Thus, the discrete shearlet transform can be rewritten as $\mathcal{SH}(\mathcal{I})(j,k,m) =$

$$\begin{cases} \texttt{ifft}(\hat{\phi}(\omega_1, \omega_2)\texttt{fft}(\mathcal{I}))(m) \\ \texttt{ifft}(\hat{\psi}_1(2^{-j}\omega_1)\hat{\psi}_2(2^{j/2}\frac{\omega_2}{\omega_1} - k)\texttt{fft}(\mathcal{I}))(m) \\ \texttt{ifft}(\hat{\psi}_1(2^{-j}\omega_2)\hat{\psi}_2(2^{j/2}\frac{\omega_1}{\omega_2} - k)\texttt{fft}(\mathcal{I}))(m) \end{cases}. \quad (6)$$

D. Computational Complexity

For an image $\mathcal{I}$ of size $N \times N$, the computational complexity of the discrete shearlet transform defined in (6) is $\mathcal{O}(SN^2 + SN^2 \log N)$, where S is the number of employed shearlets, i.e. $S = |\Psi|, \Psi = \{\hat{\psi}_{j,k} : j = 0, \ldots, j_0 - 1, -\lfloor 2^{j/2} \rfloor \leq k \leq \lfloor 2^{j/2} \rfloor\}$. Notice that S is exponential on the number of considered scales j_0. Taking into consideration that $j_0 \ll N$ and that in practice, even for high resolution images, $j_0 < 8$, we can assume S as a small constant. Therefore we conclude the computational complexity of the discrete shearlet transform is $\mathcal{O}(N^2 \log N)$ which is the computational complexity of the 2D fast Fourier transform.

Up to this point, the scalar product $\langle \mathcal{I}, \psi_{j,k,m} \rangle$ is solved in the Fourier domain by using the Plancherel formula and the 2D fast Fourier transform. A variant of this approach consists in solving the scalar product in the time domain by using 2D convolution, i.e. $\mathcal{I} * \texttt{ifft}(\hat{\psi}_{j,k,m})$. In this case the computational complexity will be $\mathcal{O}(SN^2W^2)$, where $W \times W$ is the size of the shearlets. Let consider, like in the Fourier implementation, that S is a constant and that $W \ll N$. With this assumptions, the computational complexity can be reduced to $\mathcal{O}(N^2)$. Notice that the number of considered scales j_0 is proportional to the size of the shearlets W, therefore, in order to maintain a quadratic computational complexity, we need to consider only small scales. In this case only, working in the time domain is computationally more advantageous.

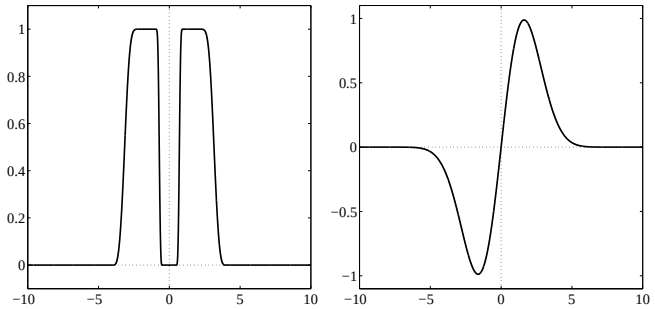

Fig. 2. Different choices for $\hat{\psi}_1$. (a) Meyer wavelet, (b) Mallat wavelet

III. Edge Detection with Shearlets

Edges are meaningful image features associated with points where the 2D signal undergoes a sharp variation. The literature on edge detection is vast and certainly out of the scope of this paper. Traditional edge detectors are based on image derivatives. A very classical algorithm is the Canny edge detector [32], which is based on three criteria for an optimal edge detection: good detection, good localization, and low spurious response. It shows that the optimal detector for an isolated step edge should be the first derivative of a Gaussian. In the Canny approach, the standard deviation σ of the Gaussian can be seen as a scale parameter which acts as a tradeoff between good localization and noise suppression. Later, Mallat and his collaborators [4], [5] generalized the Canny approach using wavelets, thus providing a multi-scale framework for edge detection in signals. In more recent years, along the rise of directional multi-scale representations, new edge detection methods based of curvelets [33], [34] and contourlets [35], have been proposed. An edge detection algorithm based on shearlets has been presented in [15], where the authors provide theoretical and numerical justifications of a cascade algorithm for edge detection.

A. Appropriate Shearlets for Edge Detection

We now discuss a possible way to exploit the shearlet transform for the estimation of edges strength and orientation. We first comment on the type of shearlets which are more appropriate for the task.

A classical choice for the function ψ_1 is the Meyer wavelet (see, for instance, [16], [36]), which is band limited and C^∞ in the frequency domain, forcing rapid decay in the spatial domain. This choice is instead not optimal for edge detection since the Meyer wavelet is an even function (see Fig 2, (a)) and thus its shearlet transforms suffer from large side-lobes around prominent edges, which interfere with the detection of the edge location, as it can be seen in the image of Fig. 3 (b).

To overcome this effect, the authors of [15] propose a discrete shearlet transform implementation that uses finite impulse response filters corresponding to the quadratic spline wavelet defined in [5]. In the latter reference it is shown that the determination of the local extrema of the wavelet transform is equivalent to Canny edge detection, provided the wavelet is

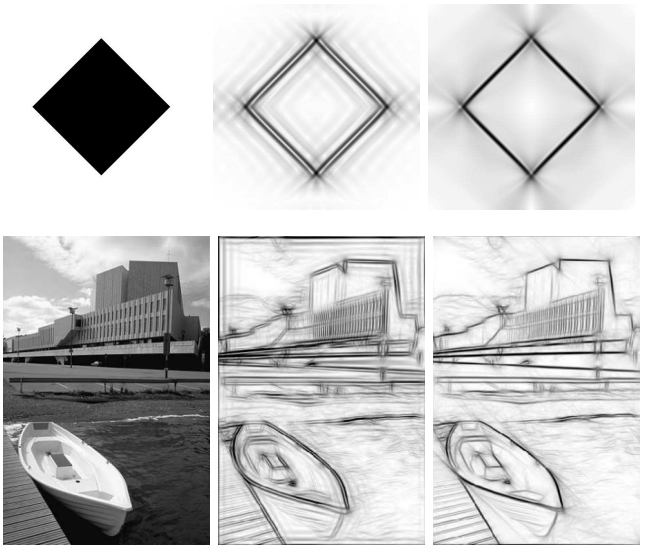

Fig. 3. Shearlet edge points. (a) Original image, (b) $\hat{\psi}_1$ chosen as the Meyer wavelet, (c) $\hat{\psi}_1$ chosen as the Mallat wavelet.

the first derivative of a Gaussian. Furthermore, the authors in [5] introduce the following family of one dimensional wavelets, namely Mallat wavelets,

$$\hat{\psi}_1(\omega) = i\omega \left(\frac{\sin(\omega/4)}{\omega/4} \right)^{2n+2}, \tag{7}$$

which share the same properties of the first derivative of the Gaussian.

In this work we obtain a shearlet suitable for edge detection, simply by replacing the Meyer wavelet with the Mallat wavelet. The effect of this change is shown in Fig. 3 (c). The Mallat wavelet is not compactly supported in the Fourier domain, however its essential support is bounded, as shown in Fig. 2 (b). As for ψ_2, instead, any smooth function with compact support in the frequency domain can be considered. In our case we used the same bump function as in [16], [36]. With this choice for ψ_1 and ψ_2, the corresponding shearlets are well localized both in frequency and time domain, see Fig. 4.

B. Multi-scale Shearlet Edge Detection

Let us consider an image $\mathcal{I}$ and address the problem of estimating the energy and orientation of candidate edges. According to the properties of the continuous shearlet transform summarized in Section II, edge points can be identified as those points $m \in \mathcal{I}$ which, at scale j, the function $\mathcal{E}_j(m)$ has large values, with

$$\mathcal{E}_j(m)^2 = \sum_k (\mathcal{SH}(\mathcal{I})(j,k,m))^2. \tag{8}$$

$\mathcal{SH}(\mathcal{I})(j,k,m)$ denotes the discrete shearlet transform of $\mathcal{I}$, as defined in Eq. (6). Fig. 5 shows the detected shearlet edge points on an example image, for different scales up to $j_0 = 4$. It can be seen that a coarse scales ($j = 0, 1$) the amount of spurious edges is lower, to the price of localization. Conversely, at fine scales ($j = 2, 3$) edge localization is very

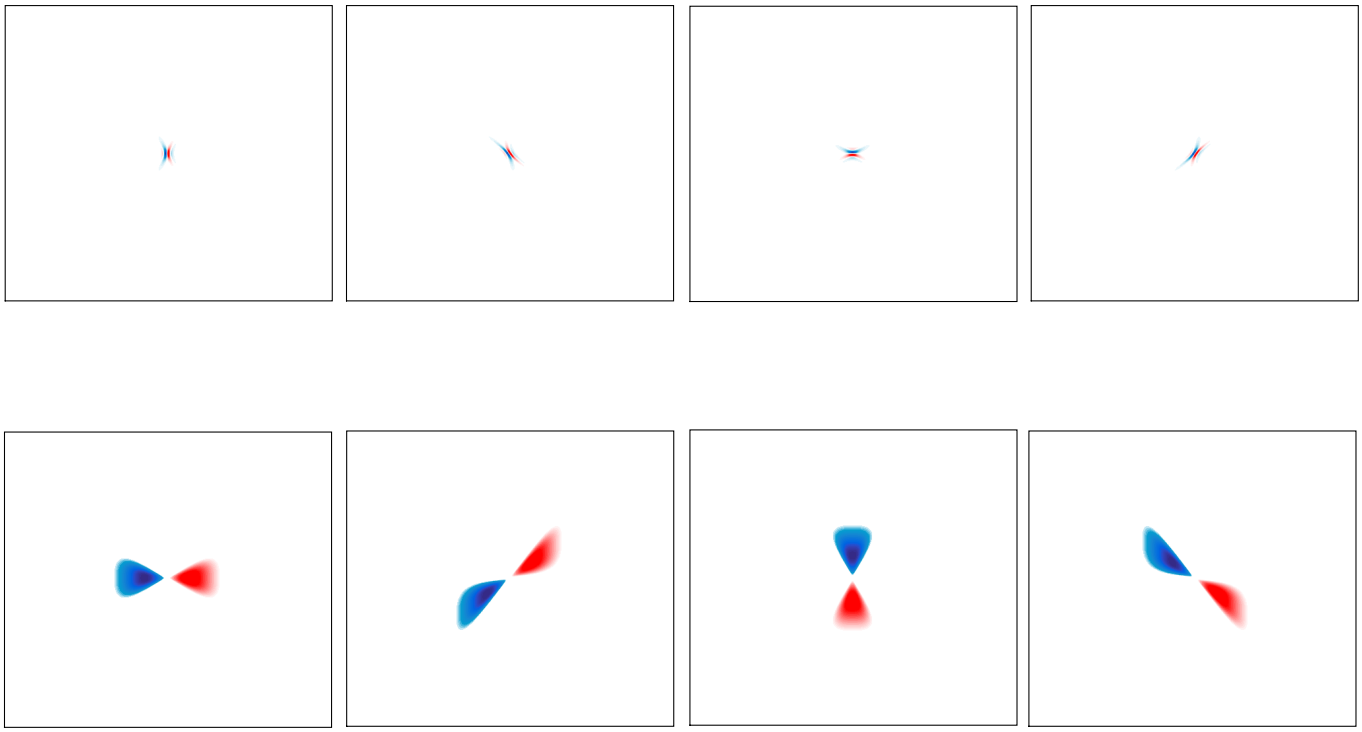

Fig. 4. Shearlets in the space (top) and frequency domain (bottom) - ψ_1 is the Mallat wavelet. Four different orientations and a fine scale ($j = 1$).

accurate, while noise increases.

Edge orientation estimation. The edge direction at a point m at scale j is easily obtained by finding the index k that maximizes $\mathcal{SH}(\mathcal{I})(j,k,m)$,

$$\theta_j(m) = \arg\max_k |\mathcal{SH}(\mathcal{I})(j,k,m)|.$$

Fig. 6 shows an example of the edge direction estimation using the shearlet transform at different scales j. The estimated directions are color coded, i.e. each color represents a specific direction summarized in the colorbar at the right of the figure. As we can observe, the shearlet transform accurately estimates the edge orientation. In addition, it can be noticed how accuracy increases at fine scales ($j \to 3$) due to the fact that at fine scales more shears k have to be considered, $-\lfloor 2^{j/2} \rfloor \leq k \leq \lfloor 2^{j/2} \rfloor$.

SCED - cascade edge energy estimation. A way to exploit multi-scale information for estimating the edge energy is to reason on the behavior of shearlet coefficients at different scales of a given point of the image.

Following the discussion of Section II (see also [4], [5]), we expect that

$$|\mathcal{SH}(\mathcal{I})(j,k,\bar{m})| \sim C 2^{-\beta j}$$

where, if $\beta \geq 0$ we may classify $\bar{m}$ as an edge point, otherwise (i.e. $|\mathcal{SH}(\mathcal{I})|$ increases at finer scales) $\bar{m}$ may be classified as noise. Based on this result, Yi et al. [15], propose a cascade algorithm that reinforces true edges and suppresses false ones. Here we propose a variant of this algorithm, summarized in Alg. 1, where `dst` is the discrete shearlet transform defined in (6), `nonmaxsup` is a non-maxima suppression function and

Algorithm 1 Shearlet cascade edge detection (SCED) algorithm. **Input** $\mathcal{I}$: input image, j_0: number of considered scales, t: threshold. **Output** $\mathcal{E}$: edge image.

procedure SCED($\mathcal{I}, j_0$)
  $\mathcal{SH} = \texttt{dst}(\mathcal{I})$;
  for all $m \in \mathcal{I}$ **do**
    $\mathcal{E}(m) = \sqrt{\sum_k (\mathcal{SH}(j_0 - 1, k, m))^2}$;
    $\theta(m) = \arg\max_k |\mathcal{SH}(j_0 - 1, k, m)|$;
  end for
  for $j = j_0 - 2, \ldots, 0$ **do**
    for all $m \in \mathcal{I}$ **do**
      $e_j(m) = \sqrt{\sum_k (\mathcal{SH}(j,k,m))^2}$;
      $\mathcal{E}(m) = \begin{cases} \mathcal{E}(m) & \text{if } \mathcal{E}(m) \leq e_j(m) \\ e_j(m) & \text{if } \mathcal{E}(m) > e_j(m) \end{cases}$
    end for
  end for
  `nonmaxsup`($\mathcal{E}, \theta$);
  `thresholding`($\mathcal{E}, t$);
  return $\mathcal{E}$;
end procedure

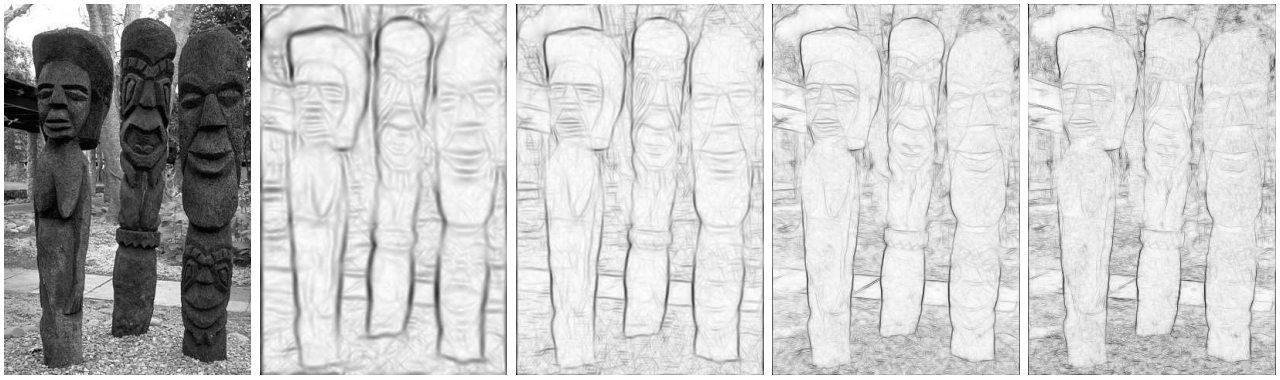

(a) Original image (b) $j = 0$ (c) $j = 1$ (d) $j = 2$ (e) $j = 3$

Fig. 5. Detected shearlet edge points at different scales j.

(a) Original image

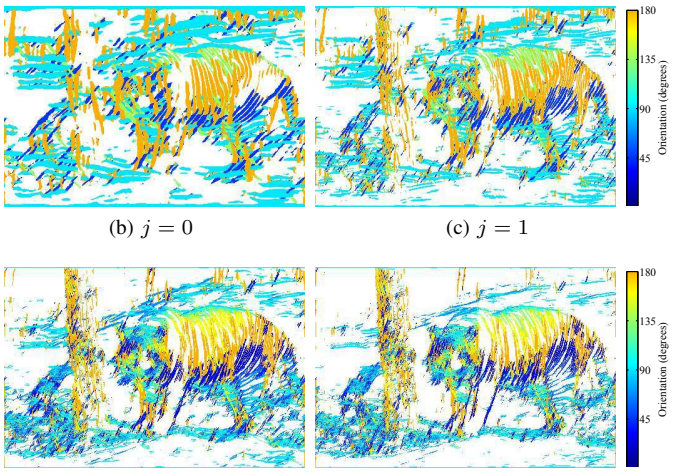

(b) $j = 0$ (c) $j = 1$

(d) $j = 2$ (e) $j = 3$

Fig. 6. Estimation of the edge direction using the shearlet transform at different scales j.

`thresholding` a function that applies a threshold to decide whether an image point is an edge or not.

We start by estimating the shearlet transform energy at the finest scale; then we correct it in all points which are likely to be noise, by applying the energy computed at coarser scales (whose coefficients are smaller in these cases). This simple procedure allows us to obtain neat results (see Fig. 7, (b)).

SMED - edge strength estimation by multiplication. Another valid approach for a multi-scale edge detector is multiplying corresponding shearlet coefficients across scales. This idea takes inspiration by Zhang et al. [22] which proposed a wavelet based edge detection scheme by scale multiplication. This idea can be easily adopted to the shearlet transform. The scale product function $\mathcal{P}$ is defined as the correlation of edge points across scales

$$\mathcal{P}(m) = \prod_{j=0}^{j_0-1} \mathcal{E}_j(m), \tag{9}$$

where $\mathcal{E}_j(m)$ are the edge candidates defined in (8).

Fig. 7 , in (b) and (d), shows the result of the cascade algorithm (SCED) and the scale multiplication algorithm (SMED) respectively. As expected, the two obtained results appear to be quite different: SCED captures edge information provided by the different scales, to the price of retaining some noise. Instead MCED returns points whose coefficients are meaningful at all the scales considered. These points correspond to very prominent edges.

The figure also reports ,in (a) and (c), the corresponding results obtained by substituting the shearlet transform with the wavelet transform described in [5]. These two algorithms are referred to as WCED and WMED respectively. As we can observe, the results of SCED and SMED are visually more pleasant that the one obtained by WCED and WMED respectively, as previously seen in [15]. In particular the edge chains are more coherent and clearly marked, and this clearly indicates the benefit of shearlets sensitivity to orientation information.

IV. Corner Detection with Shearlets

We now consider another class of image features, usually referred to as corners, which are widely used in computer vision primarily for their effectiveness in matching and tracking problems [37]. A corner can be defined as the intersection of two edges, or, as a point for which there are at least two dominant and different edge directions in a local neighbourhood of the point.

There are several approaches for detecting corners in images. Since the pioneering work of Harris and Stephens [38], and later of Shi and Tomasi [37], the structure tensor of image gradients, also known as the *autocorrelation matrix*, has become popular for corner detection. Wavelets have been applied to corner detection [6]–[8], but the corresponding algorithm is affected by the limited ability of wavelets

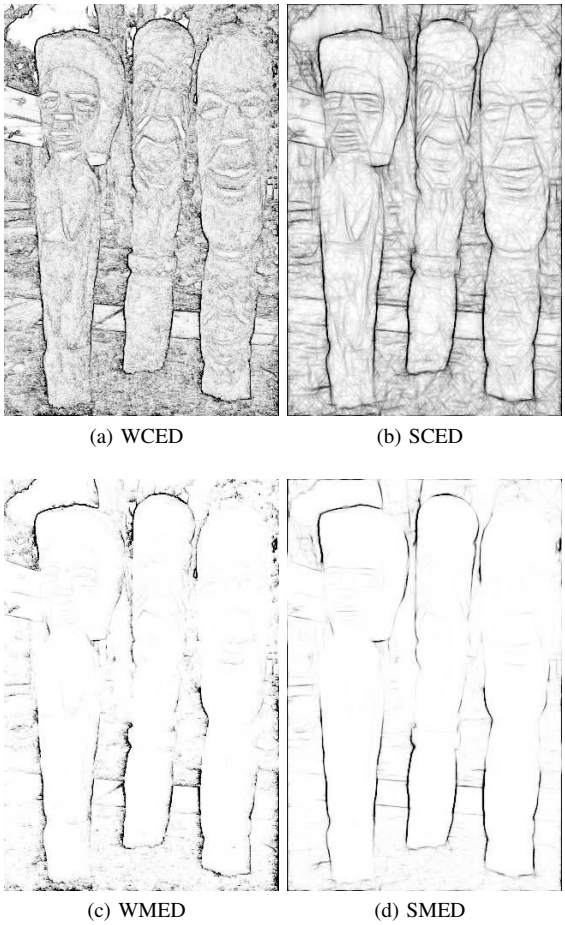

(a) WCED (b) SCED

(c) WMED (d) SMED

Fig. 7. Comparison of the cascade and scale multiplication edge detection approaches with both discrete wavelet transform and discrete shearlets transforms.

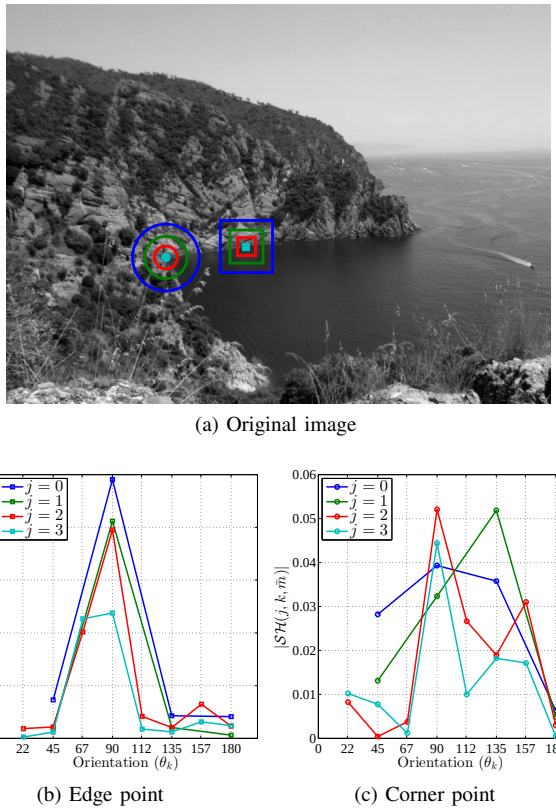

(a) Original image

(b) Edge point (c) Corner point

Fig. 8. Shearlet orientation patterns for an edge point and a corner point of a natural image.

to encode directional informations. In order to overcome this limitation, orientation sensitive wavelets, such as the Log-Gabor wavelets, can be applied [23]. Here we present an alternative way for addressing the problem effectively by selecting a more appropriate orientation selective transform. The first intuition on the applicability of shearlet transform to corner detection has been provided in [15] based on the theoretical results of [27].

SCD - shearlet corner detection. On previous sections we have discussed the ability of shearlets for detecting the directional information of edges at different scales. Therefore, its seems almost natural their use for detecting corner points. Fig. 8 shows a comparison of the orientation patterns, produced by the shearlet transform, between an edge point (square) and a corner point (circle) on a natural image. Let first analyze the orientation patterns at a fixed scale $j = 2$ (red). As we can observe, for the edge point a strong shearlet response is obtained on one direction only, while for the corner point it can be observed strong shearlet responses at two different, almost perpendicular, orientations. If we perform the analysis across scales, it can be seen how on the edge point the strongest shearlet response is maintained on one direction only across scales with the exception of the finest scale where two high responses are obtained on two close orientations. However, at the corner point, the two orientations with the strongest shearlet response slightly vary across scales. This is an expected behavior since, depending of the scale at which the analysis is performed, a corner point can have different main orientations. This example shows how, by analyzing the shearlet coefficients across shearings (orientations), corner points can be detected at different scales.

A possible way of estimating if a point is a good corner at a fixed scale is by performing a weighted sum of its shearlet coefficients across shears, where each weight is a value that represents how *perpendicular* is the orientation of the shear with the orientation of the shear with the maximum shearlet response for that point. In this way we favor points with large coefficients in at least to directions, differing about 90 degrees (the "ideal" corner). Formally, let $\mathcal{CM}$ be a *cornerness measure* estimated for a point $m \in \mathcal{I}$ and for a fixed scale j in the following way

$$\mathcal{CM}_j(m) = \sum_{u \in W(m)} \sum_{k} |\mathcal{SH}(j,k,u)| \sin(|\theta_k - \theta_{k_{\max}}|)$$

where $\mathcal{SH}(j,k,u)$ represents the discrete shearlet transform coefficient for a point u in a neighborhood of m, at scale j and shearing k, θ_k is the angle associated with the shearing k, $k_{\max} = \arg\max_k |\mathcal{SH}(j,k,m)|$ and $W(m)$ is a window centered at point m. Figure 9 shows the cornerness measure computed at different scales j. At fine scales the maxima are

very few and very local, while at coarser scales neighbouring points are also detected. For this reason a non-maxima suppression is needed [39]. Notice how edge points are seldom associated with high values, and it only happens at the coarsest scale.

SMCD - shearlet multi-scale corner detection. By aggregating the information of different scales in the following way

$$\mathcal{CM}(m) = \sum_j \mathcal{CM}_j(m)$$

we obtain a multi-scale version of the algorithm, where corners at different resolutions are detected simultaneously and detected corner points that persist across scales are reinforced. This approach is summarized in Alg. 2, where `dst` is the discrete shearlet transform defined in (6) and `nonmaxsup` is a non-maxima suppression function [39]. Notice that, unlike the non-maxima suppression defined for edge detection, this technique uses a local window sliding through all the pixels of the image. The central pixel value of the window is kept if is the local maximum within the window, otherwise is set to zero.

Automatic scale selection. Taking the advantage of the multi-scale representation produced by the shearlets, it is also possible to perform an automatic scale selection step. Therefore, the most appropriate scale $\bar{j}$ of a corner point $m \in \mathcal{C}$ is selected as

$$\bar{j} = \arg\max_j \; K_j \sum_k |\mathcal{SH}(j,k,m)|$$

where K_j is a normalization factor that depends on the scale j. Fig. 10 shows the result of the shearlet multi-scale corner detection with automatic scale selection. As we can observe, the corners detected at fine scales ($j = 2, 3$) belong to high resolution patterns like the grass, while corners detected at coarse scales ($j = 0, 1$) belong to coarse scale objects like the buildings in the background and objects out of focus.

Algorithm 2 Shearlet multi-scale corner detection (SMCD) algorithm. **Input** $\mathcal{I}$: input image, j_0: number of considered scales, t: threshold. **Output** $\mathcal{C}$: set of detected corner points.

procedure SMCD($\mathcal{I}, j_0, t$)
  $\mathcal{C} = \{\}$;
  $\mathcal{SH} = \texttt{dst}(\mathcal{I})$;
  for all $m \in \mathcal{I}$ **do**
    $\mathcal{CM}(m) = \sum_j \sum_{u \in W(m)} \sum_k |\mathcal{SH}(j,k,u)| \sin(|\theta_k - \theta_{k_{\max}}|)$;
  end for
  `nonmaxsup`($\mathcal{CM}$);
  for all $m \in \mathcal{I}$ **do**
    if $\mathcal{CM}(m) > t$ **then**
      $\mathcal{C} = \mathcal{C} \cup m$;
    end if
  end for
  return $\mathcal{C}$;
end procedure

TABLE I
EDGE ENHANCEMENT METHODS ON THE BSDS300 DATASET. RESULTS MARKED WITH (*) HAVE BEEN EXTRACTED FROM FIG 1. IN [41]

	F-measure (ODT)
Prewitt [42] (*)	0.48
Sobel [43] (*)	0.48
Roberts [44] (*)	0.47
Hildreth, Marr [45] (*)	0.50
Canny [32] (*)	0.58
Perona, Malik [46] (*)	0.56
SEW ($j = 0$) [5]	0.55
SED ($j = 0$)	**0.59**

V. EXPERIMENTAL ANALYSIS

In this section we present the experimental results of the discussed shearlet approaches for both edge and corner detection.

Edge detection. For the evaluation of the shearlet edge detection approaches we adopt the Berkeley Segmentation Dataset (BSDS300) [24], and we adopt the experimental protocol proposed in [40]. BSDS300 is a widely used benchmark for contour detection. This dataset consists of 200 very challenging natural images for training and 100 for testing. In addition, each image is associated with human-marked boundaries used as ground truth (see Fig. 11). The precision-recall curve is a parametric curve that captures the trade off between accuracy and noise as the detector threshold on the edge intensity varies. We remind *precision* is the fraction of detections that are true positives rather than false positives, that is $P = \frac{TP}{(TP+FP)}$, while *recall* is the fraction of true positives that are detected rather than missed, that is $R = \frac{TP}{(TP+FN)}$. The global F-measure, or harmonic mean of precision and recall at the optimal detector threshold, provides a summary score. The F-measure is defined as $F = \frac{2PR}{(P+R)}$. In our experiments two different quantities are reported: the best F-measure on the dataset for a fixed threshold (Optimal Dataset Threshold, ODT - referred by the acronym ODS in [41]), and the aggregate F-measure on the dataset for the best threshold in each image (Optimal Image Threshold - OIT, referred as OIS in [41]). First we report a comparative analysis with classical edge enhancement algorithms. In this analysis we consider a fixed scale scenario ($j = 0$ in our case), in order to produce a fair comparison. The results of the analysis are summarized in Table I: the shearlet-based algorithm compares favorably with the other methods, and among the others the Canny edge detector appears to be the most adequate choice.

Fig. 12 focuses on multi-scale representations: in (a) it shows the precision-recall curve for the detected edges on the BSDS300 dataset with the discrete shearlet transform (SED) and the discrete wavelet transform (WED) at different fixed scales up to $j_0 = 4$. As it can be observed, the results obtained with the discrete shearlet transform are generally better. In addition, we can see the precision increases while at the same time the recall decreases as we move from fine scales to coarse scales ($j = 3, \ldots, 0$). This is due to the fact that at coarse

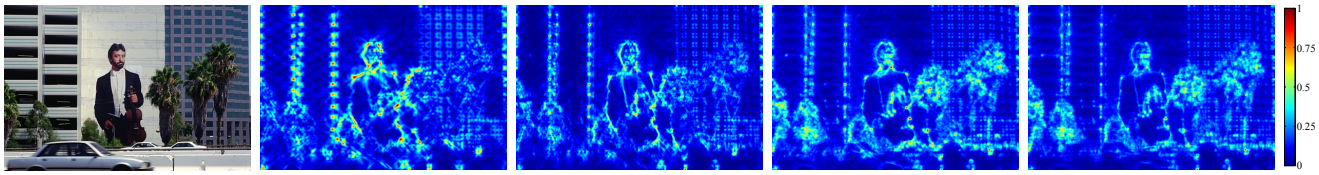

(a) Original image (b) $j = 0$ (c) $j = 1$ (d) $j = 2$ (e) $j = 3$

Fig. 9. Shearlet cornerness measure $\mathcal{CM}$ at different scales j.

(a) Original image (b) Detected corners

Fig. 10. Shearlet multi-scale corner detection (SMCD) with automatic scale selection. $j = 0$ (Blue); $j = 1$ (Green); $j = 2$ (Red); $j = 3$ (Magenta).

Fig. 11. Example images of the BSDS300. Top to Bottom: Image and ground-truth boundaries hand-drawn by different human subjects.

scales more noise is suppressed, increasing the precision and at the same time true edges can also be suppressed, therefore decreasing the recall. In theory, we should observe a similar behavior on wavelets, however at coarse scales, the edges have a noisier intensity signal. That is why with high thresholds the edges will present more discontinuities, therefore obtaining a significant drop in the precision. In Fig. 12 (b) and (c) we compare the results of the cascade algorithm (SCED) and the scale multiplication (SMED) on the BSDS300 with the output of the same methods but replacing the discrete shearlet transform with the discrete wavelet transform, denoted by WCED and WMED, respectively. We use the fast wavelet algorithm defined in Appendix B of [5] with the filters corresponding to the quadratic spline wavelet, see Table 1 of the above reference. As we can observe in both plots, SCED and SMED performs better than WCED and WMED respectively, mostly by having an increment in the precision. We remark that the main advantage of shearlets against wavelets is that we obtain an effective estimate of edge orientations.

This availability is only marginally reflected in the exdge detection algorithm, where it is used to improve the quality of the non-maxima suppression phase. Therefore it is reasonable to see a limited numerical improvement in the overall detection performances, with the positive side effect of obtaining edge maps which are cleaner and better suited for subsequent edge linking phases. Also, the obtained edge orientation map, obtained naturally with shearlets, is an important additional information to be used in higher level processing steps.

Corner detection. This evaluation is based on Mikolajczyk's software framework and image sequences[2]. Each one of the image sequences used in the evaluation contain 6 images of natural textured scenes with increasing geometric and photometric transformations. The images in a sequence are related by a homography which is provided with the image data. Fig. 13 shows the image sequences we selected for our evaluation with their respective transformation. We discarded those that are not applicable in our scenario that does not consider large zooming and rotations (normally addressed by appropriate descriptors). For the evaluation metrics we employed the number of correspondences and the repeatability score [25]. The number of correspondences $|CR_{1i}|$, is the cardinality of the set containing all the corner points correspondences between the image $\mathcal{I}_1$ and the transformed image $\mathcal{I}_i$. To calculate it, the regions representing the corner points are mapped from one image to the other using the homography. Then is checked how many of them overlap with a region from the other image by a given minimal percentage. Only corner points are taken into account that are visible in both images. On the other hand, the repeatability score RS_i for an image $\mathcal{I}_i$ is the ratio of the number of correspondences and the minimum number of corners detected in one of the images. Formally, it is defined by

$$RS_i = \frac{|CR_{1i}|}{\min\left(|\mathcal{C}_1|, |\mathcal{C}_i|\right)}$$

where $\mathcal{C}_i$ is the set of all detected corners in image $\mathcal{I}_i$.

The proposed shearlet corner detection approaches, SCD for a fixed scale j and SMCD without automatic scale selection,

[2]http://www.robots.ox.ac.uk/~vgg/research/affine/

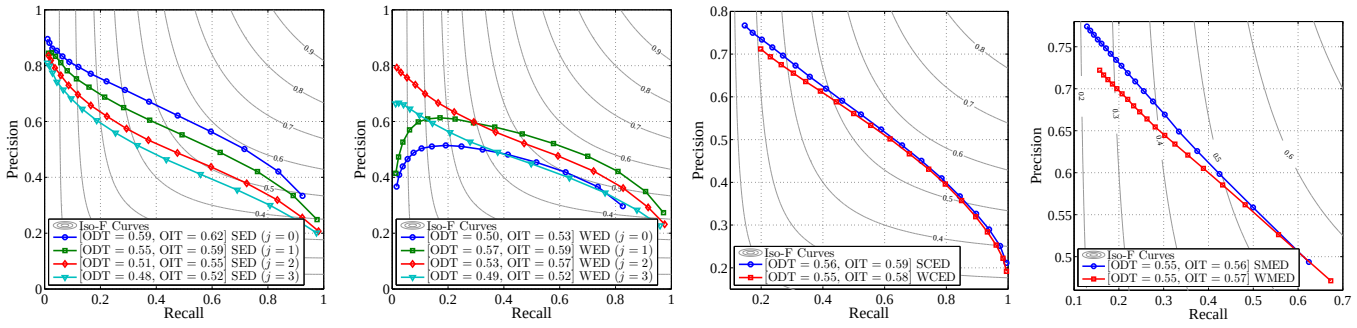

(a) (b) (c)

Fig. 12. Edge detection evaluation on the BSDS300 dataset. The F-measurements in the legend provide a summary score when an optimal threshold is selected for the entire data set (ODT) or per image (OIT). Additionally, the light gray curves represent the isolevel lines of the function $F(P, R)$.

have been compared with the classical corner detectors *Harris* [38] and *Shi-Tomasi* [37], the two methods *LGWTOI* and *LGWTSMM* proposed in [23] based on Log-Gabor wavelets, and the more recent *FAST* [47]. Automatic scale selection has not been included in the experiments for a fair comparison with the other methods. For all the methods, a threshold is established as the 10% of the cornerness measure maximum value. Detected corner points with a cornerness measure below that threshold are automatically discarded. If more than 500 detected corner points remains, only the 500 points with the maximum cornerness measure are selected. The results are reported in Fig. 14.

As we can observe in Fig. 14 (a), all corner detection methods maintain a similar repeatability score across this viewpoint angle increment, while in the number of correspondences, FAST slightly outperforms the rest. In Fig. 14 (b) in which also occurs a viewpoint change across images, the SMCD and SCD at scale $j = 2$ obtain a slightly better repeatability score and number of correspondences with respect of the rest of the corner detectors. For the image blur transformation, Fig. 14 (c) shows that Harris and LGWTSMM obtain a very high repeatability score but with the lowest number of correspondences. Shi-Tomasi and SCD at the coarsest scale $j = 0$ maintain also a high repeatability score across increasing blur but SCD at $j = 0$ outperforms Shi-Tomasi and the rest of corner detectors in the number on correspondences. In addition, the SMCD and SCD at scale $j = 1$ obtained a high number of correspondences with an acceptable repeatability score. Continuing in the image blur transformation, now in the *Trees* image sequence, Fig. 14 (d) shows how SMCD and SCD at coarse scales $j = 0, 1$ outperforms the rest of the detector in both repeatability score and number on correspondences. Finally, for the illumination change transformation, in Fig. 14 (e) can be seen how LGWTOI, FAST, SMCD and SCD at fine scales $j = 2, 3$ obtained the highest number of correspondences. While SMCD and SCD at coarse scales $j = 0, 1$ obtained the best repeatability scores.

In summary we can state that the presented shearlet approach is effective in detecting matchable corners across different image transformations and it is particularly beneficial in the case of blur and illumination changes. As for time performances, our Matlab implementation performs comparably to similar approaches who do not require a training stage [37], [38] (we refer to the performances reported in [47], Table IV): at a single scale the whole algorithm has an average of $14.2MPixel/s$, while it performs on average $16.8MPixels/s$ with pre-computed shearlets [3]. We conclude by observing that a comparative analysis with optimized libraries such as [47] would not be fair at this point, since our code has not been optimized yet and our choice of the programming language is not appropriate for this type of evaluations.

VI. Conclusions

In this paper we addressed the problem of extracting multi-scale image features, edges and corners in particular, by exploiting the shearlets framework. Shearlets are capable of capturing anisotropic information in multivariate functions and are thus particularly appropriate for the detection of directional sensitive features.

The analysis of the features across the shearlet scales allowed us to obtain meaningful features and suppress noise at the same time.

In this work we adopted an algorithm for computing the shearlet transform in the Fourier domain, the Fast Finite Shearlet Transform (FFST) [16], and chose a mother function specifically proposed in [5] for enhancing signal discontinuities. The choice allowed us to obtain computational efficiency which can be easily achieved in the frequencies domain, and a tidy implementation which follows exactly the theoretical conceptual path. We observe how interesting alternatives will be worth investigating in future works. In particular, compactly supported shearlets in the space domain [19] have been recently shown to have nice properties for edge detection [31] since they could allow us to capture effectively the spatial locality of image features.

We proposed two algorithms for multi-scale edge and corner detection, which fully exploit the expressive power of shearlets, in the enhancement of discontinuities associated with a given orientation and a given scale. The effectiveness of our contributions was substantiated by a thorough experimental analysis on benchmark datasets, where we showed

[3] Our experiments have been carried out on a 2GHz Intel i7, which is slightly superior to the processor reported in [47].

(a) *Graffiti* (viewpoint change)

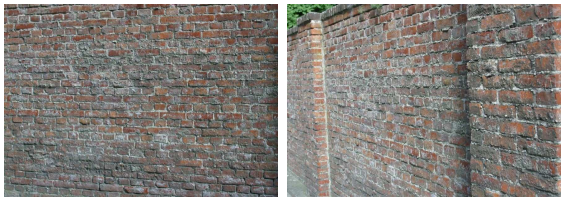

(b) *Wall* (viewpoint change)

(c) *Bikes* (image blur)

(d) *Trees* (image blur)

(e) *Leuven* (light change)

Fig. 13. Image sequences with different geometric and photometric transformations used in the corner detection evaluation.

the superiority of shearlets over wavelets for edge detection, both in quantitative and qualitative evaluations. As for corner detection, we compared our results with state of the art methods and illustrated the appropriateness of our algorithm in particular in the case of blur and illumination changes.

Future works will be devoted at extending the applicability of the general framework to the detection of other classes of image features. Furthermore, we aim to investigate the relation between our shearlet based scale selection and the other classical methods, as for example the scale-space approach, see [1] and references therein. For one-dimensional signal it is known that wavelet representation (with the derivative of the Gaussian as a mother wavelet) is equivalent to the scale-space analysis, see [48] for some further information. Our intuition is that a similar relation could also hold with shearlet. However, the parabolic scaling makes the analysis more difficult and a delicate issue is the choice of the normalization of the shearlet transform to ensure the fact that there is a unique maximum across the scale.

Acknowledgements

The authors would like to thank Demetrio Labate for many useful discussions on the subject and Nicoletta Noceti for proof reading the paper and providing useful insights. E. De Vito was partially supported by Progetto PRIN 2010-2011"Varietà reali e complesse: geometria, topologia e analisi armonica", and he is a member of the Gruppo Nazionale per l'Analisi Matematica, la Probabilità e le loro Applicazioni (GNAMPA) of the Istituto Nazionale di Alta Matematica (INdAM).

REFERENCES

[1] T. Lindeberg, *Scale-space theory in computer vision*. Kluwer Academic Publishers, 1994.
[2] S. Mallat, *A wavelet tour to signal processing*. Academic Press, 1999.
[3] P. Burt and T. Adelson, "The laplacian pyramid as a compact image code," *IEEE Transactions on Communications*, vol. 31, no. 4, 1983.
[4] S. Mallat and W. L. Hwang, "Singularity detection and processing with wavelets," *Information Theory, IEEE Transactions on*, vol. 38, no. 2, pp. 617–643, 1992.
[5] S. Mallat and S. Zhong, "Characterization of signals from multiscale edges," *IEEE Transactions on pattern analysis and machine intelligence*, vol. 14, no. 7, pp. 710–732, 1992.
[6] A. K. Chan, C. K. Chui, J. Zha, and Q. Liu, "Corner detection using spline wavelets," in *Robotics-DL tentative*. International Society for Optics and Photonics, 1992, pp. 311–322.
[7] C.-H. Chen, J.-S. Lee, and Y.-N. Sun, "Wavelet transformation for gray-level corner detection," *Pattern Recognition*, vol. 28, no. 6, pp. 853–861, 1995.
[8] F. Pedersini, E. Pozzoli, A. Sarti, and S. Tubaro, "Multi-resolution corner detection." in *ICIP*, 2000, pp. 881–884.
[9] D.-Y. Po and M. N. Do, "Directional multiscale modeling of images using the contourlet transform," *Image Processing, IEEE Transactions on*, vol. 15, no. 6, pp. 1610–1620, 2006.
[10] I. W. Selesnick, R. G. Baraniuk, and N. C. Kingsbury, "The dual-tree complex wavelet transform," *Signal Processing Magazine, IEEE*, vol. 22, no. 6, pp. 123–151, 2005.
[11] E. J. Candès and D. L. Donoho, "Ridgelets: A key to higher-dimensional intermittency?" *Philosophical Transactions of the Royal Society of London. Series A: Mathematical, Physical and Engineering Sciences*, vol. 357, no. 1760, pp. 2495–2509, 1999.
[12] E. J. Candes and D. L. Donoho, "New tight frames of curvelets and optimal representations of objects with piecewise c2 singularities," *Communications on pure and applied mathematics*, vol. 57, no. 2, pp. 219–266, 2004.
[13] D. Labate, W.-Q. Lim, G. Kutyniok, and G. Weiss, "Sparse multidimensional representation using shearlets," in *Optics & Photonics 2005*. International Society for Optics and Photonics, 2005, pp. 59 140U–59 140U.
[14] K. Guo, D. Labate, and W.-Q. Lim, "Edge analysis and identification using the continuous shearlet transform," *Applied and Computational Harmonic Analysis*, vol. 27, no. 1, pp. 24–46, 2009.
[15] S. Yi, D. Labate, G. R. Easley, and H. Krim, "A shearlet approach to edge analysis and detection," *Image Processing, IEEE Transactions on*, vol. 18, no. 5, pp. 929–941, 2009.
[16] G. S. S. Häuser, "Fast finite shearlet transform: a tutorial," *ArXiv*, no. 1202.1773, 2014. [Online]. Available: http://arxiv.org/abs/1202.1773
[17] S. Häuser and G. Steidl, "Convex multiclass segmentation with shearlet regularization," *International Journal of Computer Mathematics*, vol. 90, no. 1, pp. 62–81, 2013.
[18] D. Labate and G. R. Easley, "Image processing using shearlets," in *Shearlets: Multiscale analysis for multivariate data*, G. Kutyniok and D. Labate, Eds. Springer, 2012.
[19] P. Kittipoom, G. Kutyniok, and W.-Q. Lim, "Construction of compactly supported shearlet frames," *Constr. Approx.*, vol. 35, no. 1, pp. 21–72, 2012. [Online]. Available: http://dx.doi.org/10.1007/s00365-011-9142-y

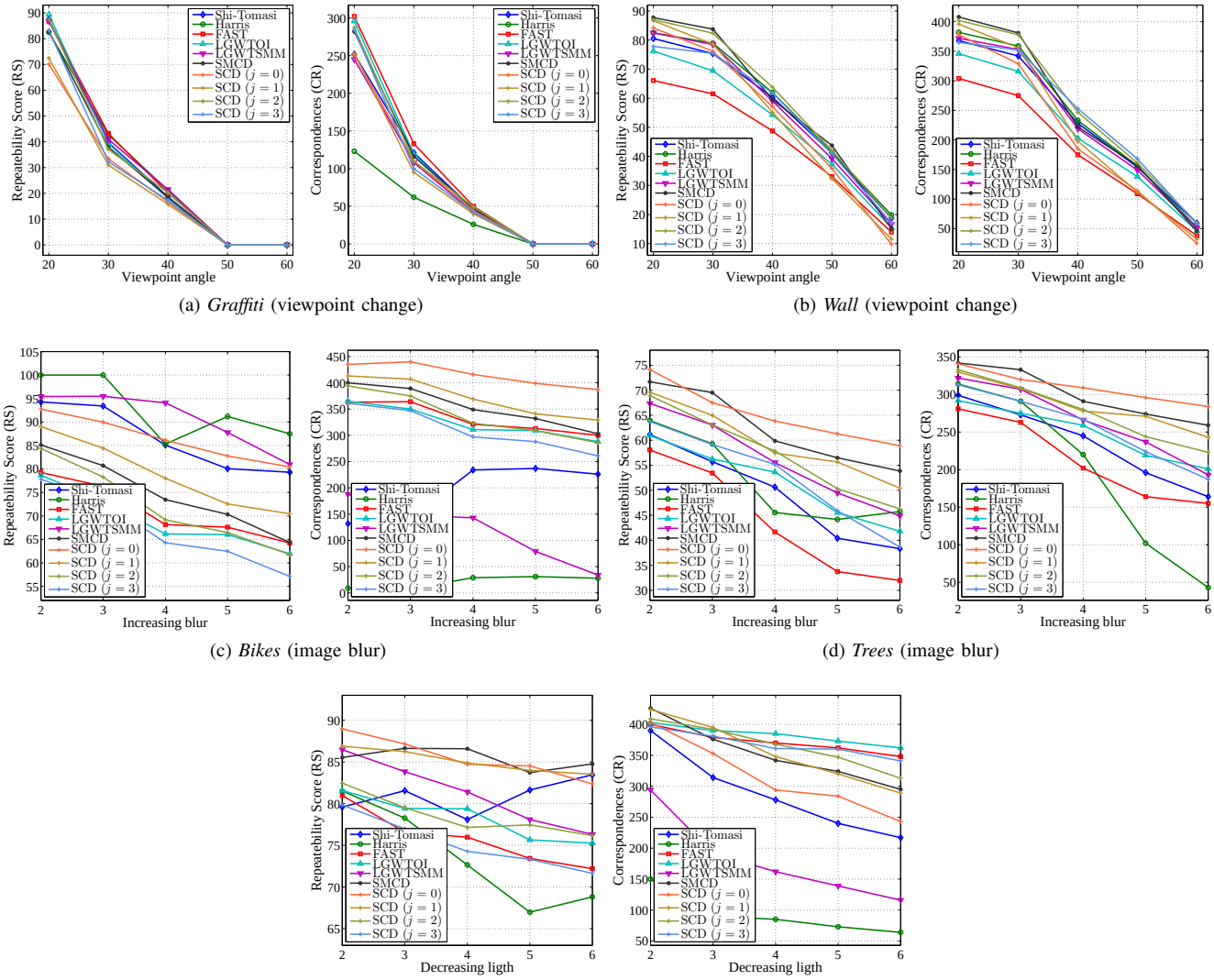

(a) *Graffiti* (viewpoint change)

(b) *Wall* (viewpoint change)

(c) *Bikes* (image blur)

(d) *Trees* (image blur)

(e) *Leuven* (light change)

Fig. 14. Comparison of different corner detectors on five image sequences.

[20] G. Kutyniok, W.-Q. Lim, and X. Zhuang, "Digital shearlet transforms," in *Shearlets: Multiscale analysis for multivariate data*, G. Kutyniok and D. Labate, Eds. Springer, 2012.

[21] G. Kutyniok, M. Shahram, and X. Zhuang, "Shearlab: A rational design of a digital parabolic scaling algorithm," *SIAM Journal on Imaging Sciences*, vol. 5, no. 4, pp. 1291–1332, 2012.

[22] L. Zhang and P. Bao, "Edge detection by scale multiplication in wavelet domain," *Pattern Recognition Letters*, vol. 23, no. 14, pp. 1771–1784, 2002.

[23] X. Gao, F. Sattar, and R. Venkateswarlu, "Multiscale corner detection of gray level images based on log-gabor wavelet transform," *Circuits and Systems for Video Technology, IEEE Transactions on*, vol. 17, no. 7, pp. 868–875, 2007.

[24] D. Martin, C. Fowlkes, D. Tal, and J. Malik, "A database of human segmented natural images and its application to evaluating segmentation algorithms and measuring ecological statistics," in *Computer Vision, 2001. ICCV 2001. Proceedings. Eighth IEEE International Conference on*, vol. 2. IEEE, 2001, pp. 416–423.

[25] K. Mikolajczyk, T. Tuytelaars, C. Schmid, A. Zisserman, J. Matas, F. Schaffalitzky, T. Kadir, and L. Van Gool, "A comparison of affine region detectors," *International journal of computer vision*, vol. 65, no. 1-2, pp. 43–72, 2005.

[26] D. Labate, W. Lim, G. Kutyniok, and W. G., "Sparse multidimensional representation using shearlets," in *Wavelets XI*. SPIE Proc. 5914, SPIE, Bellingham, WA, 2005.

[27] G. Kutyniok and D. Labate, "Resolution of the wavefront set using continuous shearlets," *Transactions of the American Mathematical Society*, vol. 361, no. 5, pp. 2719–2754, 2009.

[28] S. Dahlke, G. Kutyniok, G. Steidl, and G. Teschke, "Shearlet coorbit spaces and associated banach frames," *Applied and Computational Harmonic Analysis*, vol. 27, no. 2, pp. 195–214, 2009.

[29] G. Kutyniok and D. Labate, *Shearlets: Multiscale analysis for multivariate data*. Springer, 2012.

[30] K. Guo and D. Labate, "Characterization and analysis of edges using the continuous shearlet transform," *SIAM journal on Imaging Sciences*, vol. 2, no. 3, pp. 959–986, 2009.

[31] P. P. Gitta Kutyniok, "Classification of edges using compactly supported shearlets," *ArXiv*, no. 1411.5657, 2014. [Online]. Available: http://arxiv.org/abs/1411.5657

[32] J. Canny, "A computational approach to edge detection," *Pattern Analysis and Machine Intelligence, IEEE Transactions on*, no. 6, pp. 679–698, 1986.

[33] T. Gebäck and P. Koumoutsakos, "Edge detection in microscopy images using curvelets," *BMC bioinformatics*, vol. 10, no. 1, p. 75, 2009.

[34] G. Zhou, Y. Cui, Y. Chen, J. Yang, and H. Rashvand, "Sar image edge detection using curvelet transform and duda operator," *Electronics letters*, vol. 46, no. 2, pp. 167–169, 2010.

[35] S.-f. Ma, G.-f. Zheng, L.-x. Jin, S.-l. Han, and R.-f. Zhang, "Directional multiscale edge detection using the contourlet transform," in *Advanced Computer Control (ICACC), 2010 2nd International Conference on*,

vol. 2. IEEE, 2010, pp. 58–62.
[36] G. Easley, D. Labate, and W.-Q. Lim, "Sparse directional image representations using the discrete shearlet transform," *Applied and Computational Harmonic Analysis*, vol. 25, no. 1, pp. 25–46, 2008.
[37] J. Shi and C. Tomasi, "Good features to track," in *Computer Vision and Pattern Recognition, 1994. Proceedings CVPR'94., 1994 IEEE Computer Society Conference on*. IEEE, 1994, pp. 593–600.
[38] C. Harris and M. Stephens, "A combined corner and edge detector." in *Alvey vision conference*, vol. 15. Manchester, UK, 1988, p. 50.
[39] L. Kitchen and A. Rosenfeld, "Gray-level corner detection," *Pattern Recognition Letters*, vol. 1, no. 2, pp. 95 – 102, 1982.
[40] D. R. Martin, C. C. Fowlkes, and J. Malik, "Learning to detect natural image boundaries using local brightness, color, and texture cues," *Pattern Analysis and Machine Intelligence, IEEE Transactions on*, vol. 26, no. 5, pp. 530–549, 2004.
[41] P. Arbelaez, M. Maire, C. Fowlkes, and J. Malik, "Contour detection and hierarchical image segmentation," *Pattern Analysis and Machine Intelligence, IEEE Transactions on*, vol. 33, no. 5, pp. 898–916, 2011.
[42] J. M. Prewitt, "Object enhancement and extraction," *Picture processing and Psychopictorics*, vol. 10, no. 1, pp. 15–19, 1970.
[43] R. O. Duda, P. E. Hart *et al.*, *Pattern classification and scene analysis*. Wiley New York, 1973, vol. 3.
[44] L. G. Roberts, "Machine perception of three-dimensional soups," Ph.D. dissertation, Massachusetts Institute of Technology, 1963.
[45] E. C. Hildreth, "Edge detection," vol. 207, pp. 187–217, 1985.
[46] P. Perona and J. Malik, "Detecting and localizing edges composed of steps, peaks and roofs," in *Third International Conference on Computer Vision, ICCV 1990. Osaka, Japan, 4-7 December, 1990, Proceedings*, 1990, pp. 52–57.
[47] E. Rosten, R. Porter, and T. Drummond, "Faster and better: A machine learning approach to corner detection," *Pattern Analysis and Machine Intelligence, IEEE Transactions on*, vol. 32, no. 1, pp. 105–119, 2010.
[48] H. Führ, "Continuous diffusion wavelet transforms and scale space over Euclidean spaces and noncommutative Lie groups," in *Mathematical methods for signal and image analysis and representation*, ser. Comput. Imaging Vision. Springer, London, 2012, vol. 41, pp. 123–136. [Online]. Available: http://dx.doi.org/10.1007/978-1-4471-2353-8_7

Miguel A. Duval-Poo received the B.S degree in computer science from the University of Havana, Cuba, in 2010. He is currently pursuing the Ph.D. degree in the in the Department of Informatics, Bioengineering, Robotics, and Systems Engineering (DIBRIS), University of Genova, Italy.

His research interests include computer vision and image processing, multi-scale image representation, machine learning and multiple classifier system.

Francesca Odone Francesca Odone received a Laurea degree on Information Sciences, summa cum laude, in 1997, and a PhD in Computer Science in 2002 both from the University of Genova. She visited Heriot-Watt University (Edinburgh UK) in 1997 as a research associate and in 1999 as a visiting PhD student with a EU Marie Curie research grant.

In 2002-2005 she was a researcher at INFM (CNR). Since the end of 2005 she is Ricercatore Universitario (Assistant Professor) at the University of Genova in the Department of Informatics, Bioengineering, Robotics, and Systems Engineering. Since the end of 2014 she is Associate Professor in the same department.

She published over 60 papers on international journals and conference proceedings covering many aspects of computer vision and machine learning. Her current research interests include theory and algorithms in computer vision and machine learning, including variable selection, support set estimation, unsupervised or semi-supevised knowledge extraction from high dimensional sets; object detection and object recognition methods for images and image sequences; behaviors and actions modeling and classification; design and development of applications and prototypes for video-surveillance and biometry; study and development of computer vision methods for extracting 3D information on the observed scene.

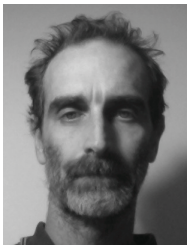

Ernesto De Vito Ernesto De Vito received a Laurea degree on Physics, summa cum laude, in 1991, and a PhD in Physics in 1995 both from the University of Genova (Italy). He visited the "Laboratoire de Physique Theorique", Universitè de Sophia Antipolis, Nice (France) in 1996 as a post-doc.

In 1997-2007 he was Assistant Professor at the University of Modena (Italy) in the Department of Mathematics. In 2007 he moved to the Department of Mathematics at University of Genova (Italy). Since the end of 2014 he is Associate Professor in the same department.

He published over 50 papers on international journals and conference proceedings on machine learning, harmonic analysis and quantum mechanics. His current research interests include the mathematical aspects of machine learning theory and the study of reproducing formulas both in the continuous and discrete framework for signal analysis.